Journal for ImmunoTherapy of Cancer

# Tumor microenvironment biomarkers predicting pathological response to neoadjuvant chemoimmunotherapy in locally advanced esophageal squamous cell carcinoma: post-hoc analysis of a single center, phase 2 study

Tingting Feng,[1] Qian Li,[2] Rui Zhu,[1] Chang Yu,[1] Liwei Xu,[3] Lisha Ying,[4] Canming Wang,[1] Weiming Xu,[5] Jinchao Wang,[1] Jing Zhu,[6] Minran Huang,[1] Chenyang Xu,[1] Jiaoyue Jin,[1] Xiaotian Zhang,[2] Tingting Lu,[1] Ying Yang,[1] Changbin Zhu,[2] Qixun Chen,[3] Dan Su [1]

**To cite:** Feng T, Li Q, Zhu R, *et al*. Tumor microenvironment biomarkers predicting pathological response to neoadjuvant chemoimmunotherapy in locally advanced esophageal squamous cell carcinoma: post-hoc analysis of a single center, phase 2 study. *Journal for ImmunoTherapy of Cancer* 2024;**12**:e008942. doi:10.1136/jitc-2024-008942

► Additional supplemental material is published online only. To view, please visit the journal online (https://doi.org/10.1136/jitc-2024-008942).

TF, QL and RZ contributed equally.

Accepted 09 August 2024



For numbered affiliations see end of article.

**Correspondence to**
Dr Qixun Chen; chenqx@zjcc.org.cn

Dr Dan Su; sudan@zjcc.org.cn

## ABSTRACT

**Background** Neoadjuvant chemoimmunotherapy has a promising effect on locally advanced esophageal squamous cell carcinoma (ESCC). However, reliable biomarkers robustly predicting therapeutic response are still lacking.

**Methods** Formalin-fixed and paraffin-embedded pre-neoadjuvant chemoimmunotherapy biopsy samples from locally advanced ESCC patients were collected. Cohort 1 composed of 66 locally advanced ESCC patients from a prospective clinical trial (NCT04506138) received two cycles of camrelizumab in combination with nab-paclitaxel and carboplatin every 3 weeks. Cohort 2 included 48 patients receiving various types of immune checkpoint inhibitors with (nab-)paclitaxel and platinum-based chemotherapy as neoadjuvant therapy. Cohort 3 consisted of 27 ESCC patients receiving neoadjuvant treatment of toripalimab with chemotherapy and was used as the external validation dataset. Targeted RNA sequencing, immunohistochemistry for programmed death ligand 1 (PD-L1), and multiplex immunofluorescence (mIF) imaging were performed.

**Results** Integration of targeted RNA sequencing, PD-L1 immunohistochemistry, and mIF revealed a significant immune-suppressive microenvironment with higher neutrophil infiltration, enriched TGF-β, and cell cycle pathways in non-pathological complete response (non-pCR) patients. NK, activated $CD4^+$ T cell infiltration, interferon-gamma, antigen processing and presentation, and other immune response signatures were significantly associated with pCR. Based on discovered tumor microenvironmental characteristics and their closely related genes were screened. Consequently, a seven-gene neoadjuvant chemoimmunotherapy risk prediction signature (NCIRPs) model, was constructed. In addition to cohort 1, this model alone or with PD-L1-combined positive score (CPS) demonstrated a higher prediction accuracy of pathological response than PD-L1 CPS or other routinely used immune signatures, such as IFN-γ, in cohorts 2 and 3. Neither prognostic association nor correlation with response to chemoradiotherapy was observed in The Cancer Genome Atlas Program ESCC dataset or in ESCC patients in the neoadjuvant chemoradiotherapy cohort (cohort 4).

### WHAT IS ALREADY KNOWN ON THIS TOPIC

⇒ Over half of locally advanced esophageal squamous cell carcinoma (ESCC) patients do not achieve major pathological response and pathological complete response (pCR). The absence of reliable biomarkers for neoadjuvant chemoimmunotherapy underscores the importance of accurately predicting its efficacy and identifying patients who will benefit.

### WHAT THIS STUDY ADDS

⇒ Immunosuppressive microenvironment, including tumor-associated neutrophil type 2 and TGF-β pathway, is revealed in the non-pCR subgroup and is associated with immunotherapy resistance. Comprehensive scoring system combining features of immunosuppressive and pro-inflammatory microenvironment can better define the patient's immune status and treatment benefit putatively guiding clinical decision for neoadjuvant treatment of locally advanced ESCC.

### HOW THIS STUDY MIGHT AFFECT RESEARCH, PRACTICE OR POLICY

⇒ The neoadjuvant chemoimmunotherapy risk prediction signature model can screen potentially beneficial patients for immunotherapy, optimize clinical treatment plans for ESCC patients, and improve overall patient survival and prognosis.

**Conclusion** The NCIRPs model that was developed and validated using treatment-naïve endoscopic samples from the largest ESCC neoadjuvant chemoimmunotherapy dataset represents a robust and clinically meaningful approach to select a putative responder for neoadjuvant chemoimmunotherapy in locally advanced ESCC patients.

## INTRODUCTION

Although locally advanced esophageal squamous cell carcinoma (ESCC) is often treated with preoperative neoadjuvant chemoradiotherapy (nCRT) followed by surgery, the 5-year survival rate lingers at 50%, and some patients suffer from toxicity-related morbidity without benefitting from nCRT.[1 2] There is a pressing need to explore more effective neoadjuvant strategies, especially for patients with multi-station lymph node metastases, who face increased perioperative complications after neoadjuvant chemoradiation.

Immune checkpoint inhibitors (ICIs), particularly programmed cell death protein 1/programmed cell death ligand 1 (PD-1/PD-L1) inhibitors like pembrolizumab,[3] nivolumab,[4] camrelizumab,[5] toripalimab,[6] sinilimab,[7] and tislelizumab,[8] have significantly improved treatment outcomes for advanced ESCC when combined with chemotherapy. This approach has become a guideline recommendation for metastatic ESCC patients, as evidenced by studies like CheckMate-577, which has shown nivolumab nearly doubling median disease-free survival to 22.4 months.[9] These findings lay the foundation for neoadjuvant chemoimmunotherapy for ESCC treatment. Several prospective studies have further demonstrated that neoadjuvant ICIs in combination with conventional chemotherapy can enhance the R0 resection rate (80.5%–100%) due to high pathological complete response (pCR) (18.8%–46.2%) and major pathological response (MPR) (43.8%–69.2%), with manageable treatment-related adverse events (18.3%–42.2%) and no mortality within 30 and 90 days postoperatively.[10–15] Thus, neoadjuvant chemoimmunotherapy is promising for locally advanced esophageal cancer.

However, the fact that over half of locally advanced ESCC patients do not achieve MPR and pCR cannot be overlooked. The absence of reliable biomarkers for neoadjuvant chemoimmunotherapy underscores the importance of accurately predicting its efficacy and identifying patients who will benefit. PD-L1 expression is a common[3 4] but not perfect biomarker for chemoimmunotherapy in advanced ESCC.[6] Recent advances in high-throughput sequencing have identified tumor microenvironment (TME) subtypes as potential generalized immunotherapy biomarkers across various cancers.[16] Comprehensive analyses have classified ESCC into four molecular subtypes, with immune modulation subtypes showing increased sensitivity to ICIs.[17] Despite these insights, the application of gene expression profiles (GEPs) based on formalin-fixed paraffin-embedded (FFPE) tissue samples, especially on treatment-naïve endoscopic biopsies, to predict neoadjuvant chemoimmunotherapy efficacy in ESCC remains unexplored and challenging.

The present study analyzed three neoadjuvant chemoimmunotherapy cohorts and one neoadjuvant chemoradiotherapy cohort. In cohort 1, 66 patients in a prospective clinical trial (NCT04506138) received two cycles of camrelizumab in combination with nab-paclitaxel and carboplatin every 3 weeks. In cohort 2, 48 patients received various types of ICIs with (nab-) paclitaxel and platinum-based chemotherapy as neoadjuvant therapy. In cohort 3, 27 ESCC patients received neoadjuvant toripalimab with chemotherapy and were used as the external independent validation cohort. In cohort 4, 28 ESCC patients underwent chemoradiotherapy as the neoadjuvant treatment. In cohorts 1, 2, and 4, 66, 48, and 28 FFPE treatment-naïve endoscopic specimens from locally advanced ESCC patients receiving chemoimmunotherapy and chemoradiotherapy were analyzed, respectively. Targeted RNA sequencing of 2402 immune-oncology genes was employed to evaluate TME and cancer cell hallmarks based on FFPE-derived RNA. Transcriptional data were publicly available in cohort 3.[15] The study aims were to (1) identify immune landscape patterns and key molecular characteristics to differentiate patient sensitivity and resistance to neoadjuvant chemoimmunotherapy, and (2) construct risk prediction signatures based on FFPE samples to guide patient selection for neoadjuvant chemoimmunotherapy.

## STAR METHODS

### Participants and sample collection

Patients with locally advanced ESCC were recruited from Zhejiang Cancer Hospital (Hangzhou, China) between January 1, 2020 and May 30, 2022. Patient inclusion criteria were as follows: (1) receipt of neoadjuvant chemoimmunotherapy comprising two 21-day cycles of paclitaxel/albumin paclitaxel, cisplatin/carboplatin, and anti-PD-1/anti-PD-L1 antibodies; and (2) surgical resection of the primary ESCC lesion within 6–9 weeks after the first neoadjuvant chemoimmunotherapy treatment. Two cohorts of locally advanced ESCC with a total of 114 patients were included in the study. Overall, 114 pre-neoadjuvant chemoimmunotherapy endoscopic biopsy FFPE specimens were collected from patients with locally advanced resectable ESCC. Cohort 1 consisted of 66 samples from patients receiving camrelizumab (200 mg on day 1, every 3 weeks) in combination with paclitaxel for injection (albumin-bound; 100 mg/m2 on days 1 and 8, every 3 weeks) and carboplatin (AUC5 on day 1, every 3 weeks) based on a prospective clinical trial (NCT04506138). Cohort 2 included 48 samples from real-world patients receiving various types of ICIs combined with paclitaxel and platinum-based chemotherapy. Detailed patient information is provided in figure 1, online supplemental tables S1 and S2. Cohort 4 comprised 28 samples focused on assessing the effectiveness of nCRT followed by surgery in patients with locally advanced ESCC (https://clinicaltrials.gov/ct2/show/NCT03381651). Histomorphology

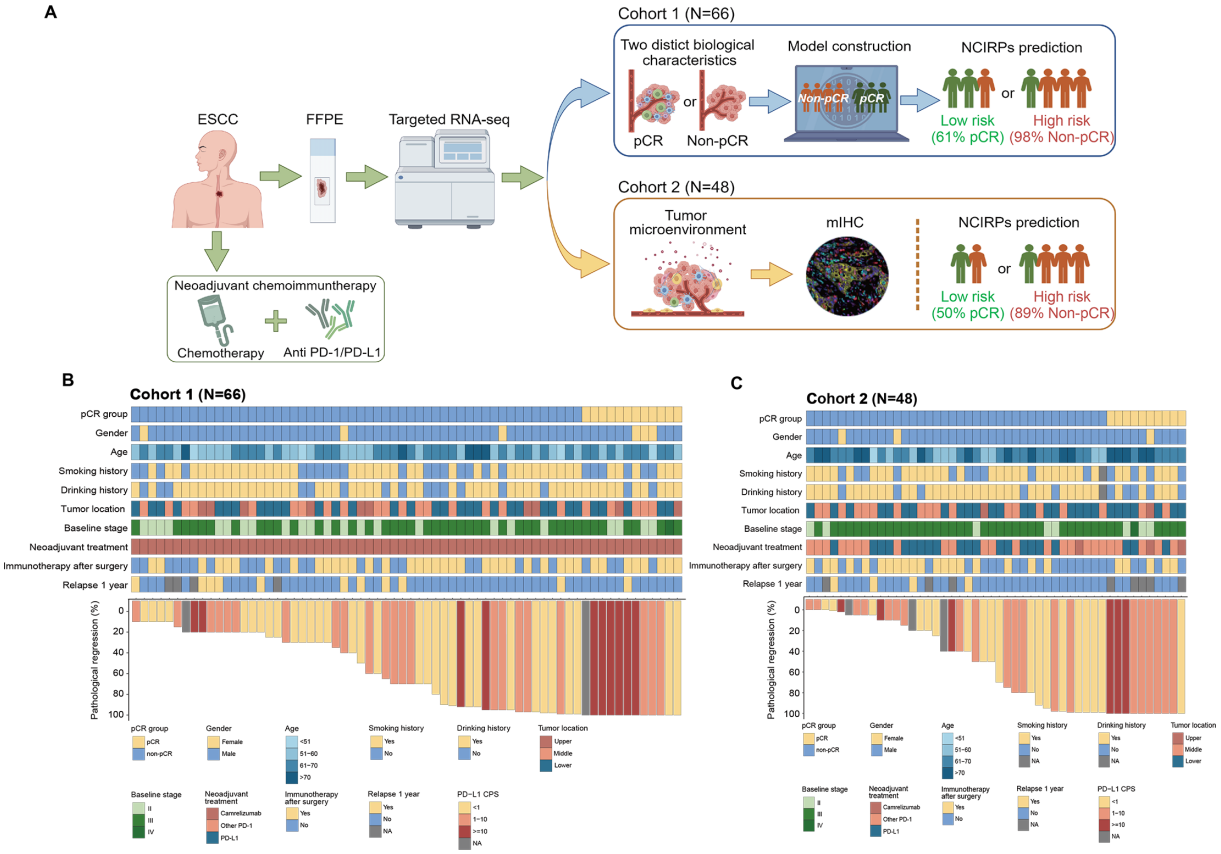


**Figure 1** Schematic illustration of study design and baseline characteristics of patients. (A) Schematic illustration of study design, by Figdraw. Total of 114 patients from Zhejiang Cancer Hospital treated between 2020 and 2022 were included. All formalin-fixed paraffin-embedded (FFPE) esophageal squamous cell carcinoma samples were subjected to RNA expression profiling via targeted RNA sequencing. Patients were divided into cohorts 1 (N=66) and 2 (N=48). (B–C) Heatmaps illustrating baseline characteristics of cohorts 1 (N=66) and 2 (N=48).

and regression grading were assessed using the Becker Grading Criteria. Tumor response and time to progression for each patient were evaluated according to the Response Evaluation Criteria in Solid Tumors version 1.1. The last follow-up date for the study was in September 2022.

## RNA extraction and library preparation

Total RNA was extracted from FFPE tumor samples using the AmoyDx FFPE RNA Extraction Kit (Cat. # 8.02.24101X036G, AmoyDx, Xiamen, China). RNA concentration was quantified using a Qubit fluorometer (Thermo Fisher Scientific, Waltham, MA, USA). Fragment length was assessed using the Agilent 2100 Bioanalyzer and RNA HS Kit (Cat. # 5067-1511, Agilent Technologies, Santa Clara, CA, USA). RNA fragmentation was performed by subjecting the samples to a temperature of 95°C for 0–15 min based on the DV200 value estimated by the Agilent 2100 Bioanalyzer System. The fragmented RNA was then reverse transcribed, and complementary DNA synthesis and strand-specific library preparation were performed using the NEBNext Ultra II Directional RNA Library Prep Kit for Illumina (Cat. # E7760L, NEB, Beverly, MA, USA).

## Hybrid capture and sequencing

RNA libraries were captured using the AmoyDx Master Panel (Cat. # 8.06.0130, AmoyDx, Xiamen, China) for RNA expression detection and sequenced on the Illumina NovaSeq 6000 platform (San Diego, CA, USA).

## Gene expression estimation

Paired-end RNA-seq reads were mapped to the *Homo sapiens* genome assembly GRCh37 (hg19) using STAR 32 (version 020,201)[18] and transcriptome annotation from Genecode version 20. Gene quantification was performed using RSEM 33 (version v1.2.28).[19] Transcripts per kilobase million (TPM) values at the gene level were calculated by counting coding region reads while considering the different types of library preparation.

## Differential gene expression and pathway analysis

Wilcoxon rank-sum test, a classical non-parametric statistical test, was used to compare gene expression levels between two conditions.[20] Differentially expressed genes (DEGs) were identified based on the following criteria: genes with fold change ≥1.5 and $p<0.05$ for the comparison between pCR and non-pCR. ESTIMATE enrichment analyses were conducted using the R package "clusterProfiler"[21] to determine the functional roles of DEGs.

These included Gene Ontology, Kyoto Encyclopedia of Genes and Genomes, Hallmark, Wikipathway, and Reactome. Gene sets were obtained from the human Molecular Signatures Database.[22] Previously identified tumor-associated neutrophil phenotype signatures[23 24] were used to distinguish antitumor N1 tumor-associated neutrophils (TAN1) from tumor-promoting N2 tumor-associated neutrophils (TAN2).

### Evaluation of TME

The single-sample gene set enrichment analysis algorithm was used to evaluate the relative abundance of infiltrating immune cells in the TME of ESCC.[25] Gene sets for TME-infiltrating immune cells were extracted from previous datasets.[16 26] Enrichment scores calculated using the R package "GSVA" were used to determine the relative abundance of each TME-infiltrating cell in ESCC.[27]

### Screening of key genes and construction of risk prediction model

Univariate logistic regression analysis was performed to calculate the OR and 95% CI for the association between DEG expression and probability of achieving pCR. Gene sets that exhibited stable differential expression and had a p<0.05 in the logistic regression results were defined as key genes. Based on these key gene sets, the least absolute shrinkage and selection operator (LASSO) method was used to further reduce the feature genes and finally select the hallmark relevant genes to establish a multivariable risk model for predicting patient response to neoadjuvant chemoimmunotherapy. The risk score for each patient was calculated as follows: Risk score=$\Sigma[A_i*\log_2(TPM+1)(Gene_i)]$ (i=1, 2, 3, …, n). The optimal model was evaluated via (1) the balance between gene numbers and the area under the receiver operating characteristic (ROC) curve (AUC) in cohort 1; (2) the validation result in cohort 2 with AUC more than 0.75.[28–30]

### Multiplex immunofluorescence

Three cases of pretreatment biopsy specimens from each of the pCR and non-pCR groups (patients with more than 30% tumor cell residual) were selected for multiplex immunofluorescence (mIF) staining in cohort 2 (figure 1A). Tissue sections with a thickness of 5 µm were prepared and mounted on adhesion microscope slides. The slides underwent deparaffinization, rehydration, and antigen retrieval for mIF staining, which were carried out using the TG TSA Multiplex IHC Assay Kits (TGMSCC1050, TissueGnostics Asia-Pacific). Staining for DAPI (TG470SN, TissueGnostics), panCK (zm-0069, ZSGB-BIO), CD66b (ab300122, Abcam), CD15 (ab172729, Abcam), ARG1 (ab133543, Abcam), INHBB (ab69286, Abcam), and HSPA2 (ab108416, Abcam) was conducted to characterize the TME and molecular features of responders and non-responders. Quantification of cell density, nucleus area per cell, area per cell, and expression per cell was performed using StrataQuest software (V.7.1.129, TissueGnostics GmbH, Vienna, Austria). Visualization of different fluorophores was achieved using the TissueFAXS Spectra Systems (TissueGnostics) and StrataQuest analysis software (V.7.1.129, TissueGnostics). Additional methodological details can be found in the article by Zhang *et al*.[31]

### Public dataset

Gene expression and clinical data for external validation cohort (cohort 3), and The Cancer Genome Atlas (TCGA)-ESCC are included within the published article and its supplementary information files.[15]

### Statistical analysis

Demographic characteristics of patients were summarized using descriptive statistical methods. $\chi^2$ or Fisher's exact probability tests were used to compare rates or percentages for significance. Non-parametric Wilcoxon rank-sum tests were used to compare medians between two datasets. Analysis of variance tests were conducted for comparisons among three or more groups. ROC-AUC analysis was performed using the R package "pROC". All statistical analyses were conducted using R Project (V.4.1.2; https://www.r-project.org/). P<0.05 was considered statistically significant.

## RESULTS

### Overview of patient cohorts

The present study retrospectively enrolled patients with ESCC undergoing neoadjuvant chemoimmunotherapy. Cohort 1 consisted of 66 patients treated with two cycles of camrelizumab combined with paclitaxel (albumin-bound) and carboplatin between January 1, 2020 and May 30, 2022 (figure 1B). Cohort 2, which was retrospectively assembled between June 2020 and July 2022, included 48 patients (figure 1C). They received two cycles of neoadjuvant chemoimmunotherapy of paclitaxel or paclitaxel for injection (albumin-bound) and platinum or carboplatin in combination with durvalumab (21 cases), sinilimab (10 cases), pembrolizumab (seven cases), tislelizumab (five cases), camrelizumab (three cases), nivolumab (one case), and toripalimab (one case).

In cohort 1 (NCT04506138), the median age was 62.0 years, with females constituting 9.1% of the cohort population. With 20 months of median follow-up, 18.2% of patients reached pCR. The 1-year relapse rate stood at 16.7% (figure 1B, online supplemental table S1).

In cohort 2, the median age was 66.5 years, with females making up 6.3% of the cohort population. Median follow-up was 18.1 months, with 20.8% of patients achieving pCR. The 1-year relapse rate was 8.3% (figure 1C, online supplemental table S2).

All 27 patients in cohort 3 were treated with a combination of toripalimab, albumin paclitaxel, and S-1, with 29.6% achieving pCR. The median age was 58.0 years, with females representing 14.8% of the patient population. The 1-year relapse rate was 18.5% (online supplemental figure S4A).

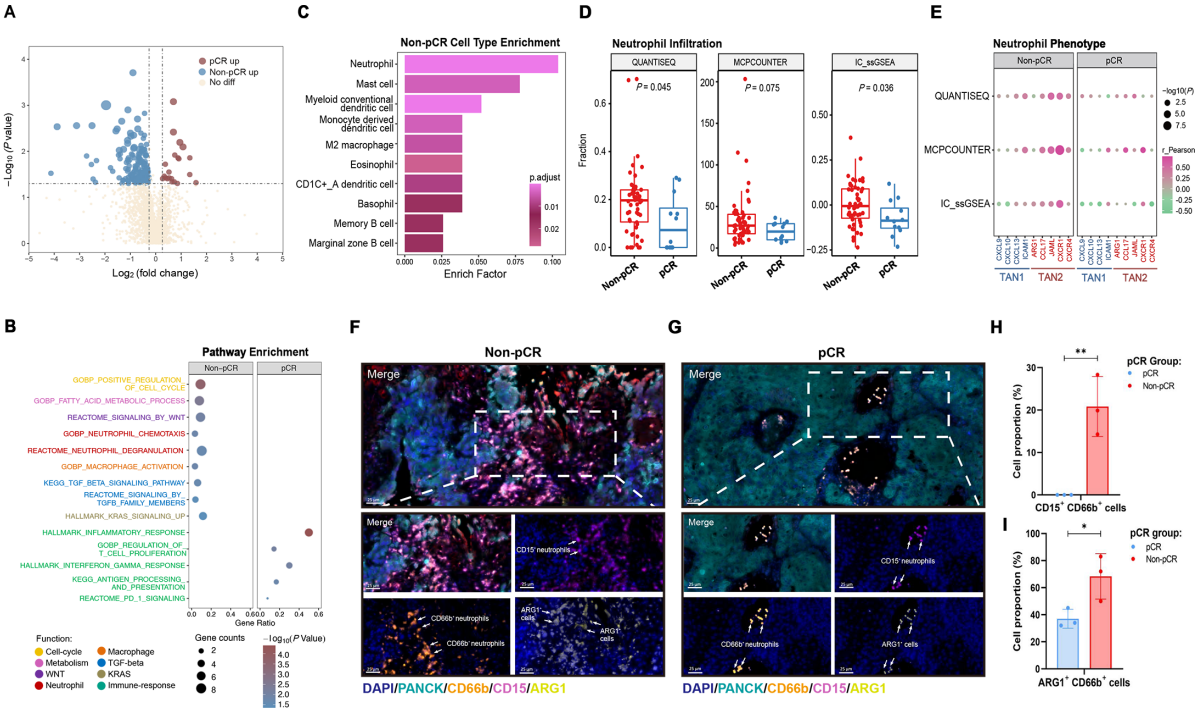


**Figure 2** Neutrophil-enriched tumor microenvironment phenotype in non-pCR patients. (A) Differential gene expression analysis based on pCR in cohort 1 (fold change >1.5, p<0.05). Red points on the right side represent highly expressed genes in pCR, while blue points on the left represent highly expressed genes in non-pCR. Dot size indicates the absolute value of the fold change and p value. (B) Results of pathway enrichment under different therapeutic responses in cohort 1. (C) Gene Set Enrichment Analysis (GSEA) of differentially expressed genes based on Gene Ontology Cellular Component (GO-CC) biological process enrichment. (D–E) Enrichment results of neutrophil infiltration and neutrophil phenotype-related genes between the non-pCR and pCR groups within cohort 1 obtained using different methods. (F–G) Representative multiplex immunofluorescence images of patients in cohort 2. Nuclei (DAPI, blue), PANCK (green), CD66b (orange), CD15 (pink), ARG1 (yellow). (H–I) Proportion of different cells in patients with different therapeutic responses in cohort 2. *, **, and *** represent p<0.05, p<0.01, and p<0.001, respectively. pCR, pathological complete response; TANs, tumor-associated neutrophils; TAN1, antitumoral TAN; TAN2, protumoral TAN.

## Pretreatment immunosuppressive microenvironment as a hallmark in non-pCR patients

Total 111 DEGs were identified, 14 DEGs in pCR and 97 DEGs in non-pCR (figure 2A). Pathway enrichment results showed that in non-pCR ESCC patients, pathways such as the cell cycle, fatty acid metabolism, Wnt signaling, neutrophil activity, macrophage activation, and the TGF-beta signaling pathway were prominently enriched. In contrast, the pCR group of ESCC patients also showed significant enrichment in pathways including the KRAS signaling, inflammatory response, T cell proliferation, interferon-gamma, antigen processing and presentation and the PD-1 signaling pathway (figure 2B).

Of note, neutrophil recruitment (CCL14/17/19) and degranulation (ARG1), together with over-presentation of cell-cycle (CDC25B), TGF-β super-family (INHBB) were disclosed (figure 2B, online supplemental table S3). Similar biological features were also recapitulated in cohort 2 (online supplemental figure S1A). Further, in cohorts 1 and 2, neutrophils, especially TAN2, immunosuppressive cells that have been implicated in immunotherapy resistance,[24] were enriched in the non-pCR subgroup (figure 2C–E, online supplemental figure S1B). Of the increasingly infiltrated TAN2 was also supported by the mIF in non-pCR patients (cohort 2) (figure 2F–I).

Besides, as an important TGF-β-related gene, tumor-derived INHBB was upregulated in non-pCR ESCC and was negatively correlated with CD274 (PD-L1) (online supplemental figure S2A–F).

These results highlighted TAN2 infiltration characterized by ARG1 overexpression, enriched TGF-β superfamily with high expression of INHBB and cell-cycle, featured by CDC25B over-presentation, might be hallmarks contributing to an immunosuppressive microenvironment resulting poor response to neoadjuvant chemoimmunotherapy.

## Pro-inflammatory TME as a hallmark of ESCC patients with pCR

The enrichment pathway of cancer hallmarks from the Molecular Signatures Database between pCR and non-pCR patients showed that patients who achieved pCR showed significant activation of pro-inflammatory pathways, including inflammatory response, regulation of T cell proliferation, antigen processing and presentation, PD-1 signaling (figure 2B) and enrichment

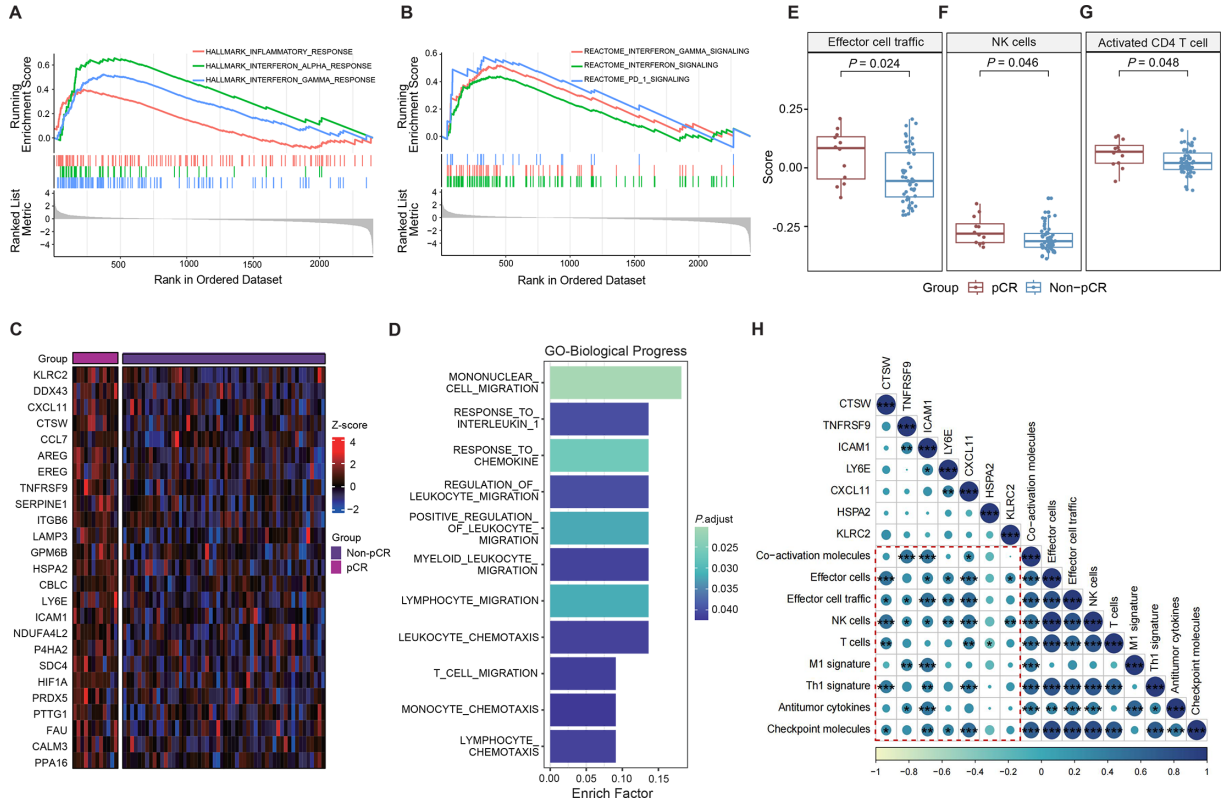


**Figure 3** Immune-enriched tumor microenvironment phenotype in responsive patients. (A–B) Enriched GSVA items in Hallmark and Reactome. (C) Heatmap of the cohort 1 showing highly expressed genes in responsive patients. (D) Results of Gene Ontology Biological Process enrichment. (E–G) Boxplots illustrating the fraction of different immune cells in patients with different responses in the cohort 1. (H) Correlation heatmap analyzing the association of genes with gene expression signatures in 29Fges (cohort 1). Dot size represents the absolute value of the correlation coefficient, dot color represents the Pearson correlation coefficient. *, **, and *** represent p<0.05, p<0.01, and p<0.001, respectively.

of IFN-γ, α pathway (figures 2B and 3A,B). Further analysis of pCR related DEGs (figure 3C) revealed increased enrichment of immune cell chemotaxis (figure 3D). In parallel, signatures of infiltrated NK and $CD4^+$/effector T cell were notably overexpressed in the pCR group, including activated $CD4^+$ T cells (p=0.048), NK cells (p=0.046), and effector cell traffic (p=0.024) (figure 3E–G). The correlation analysis indicated following genes (CTSW, TNFRSF9, ICAM1, LY6E, CXCL11, HSPA2, and KLRC2) were significantly associated with pro-inflammatory TME (figure 3H), suggesting potential roles resulting favorable response to neoadjuvant chemoimmunotherapy.

### Construction of a seven gene prediction model based on the hallmarks of response to neoadjuvant chemoimmunotherapy

The preceding analysis and pathway enrichment results indicated that differentially expressed genes associated with the cell cycle, neutrophil, and TGF-β signaling were markedly enriched in non-pCR patients (figure 2B, online supplemental table S3). And those involved in inflammatory response, T cell functions, IFN-γ signaling, antigen processing and presentation, and PD-1, were predominantly enriched in pCR patients (figure 2B, online supplemental table S3).

To translate these biological and microenvironmental hallmarks into a putative tool evaluating the response of chemoimmunotherapy in clinical practice, logistic and LASSO regression analyses were used to identify potential genes predictive of neoadjuvant chemoimmunotherapy response (figure 4A,B). 15 genes were screened out closely relating to the therapeutic response (figure 4C). Notably, these genes linked to immune response, neutrophils, TGF-β signaling, and cell cycle were highlighted as potential predictors. Finally, seven genes were selected based on the defined hallmarks of therapeutic response, and a model with non-inferior performance to the 15 genes was constructed (online supplemental figure S3). Notably, within this gene set, ARG1 for TAN2, INHBB for TGF-β superfamily, CDC25B for cell cycle represented immune-suppressive hallmarks, and gene set of LY6E, TNFRSF9, HSPA2, CTSW indicated pro-inflammatory response (figure 4D, online supplemental table S4). And a linear model termed the neoadjuvant chemoimmunotherapy risk prediction signature (NCIRPs) was constructed with the optimal performance in cohort 1.

The optimal cut-off was determined using cohort 1 (figure 4E). The NCIRPs demonstrated outstanding performance in both cohorts 2 (AUC=0.855) and 3 (AUC=0.771) (figure 4F,G). However, no difference

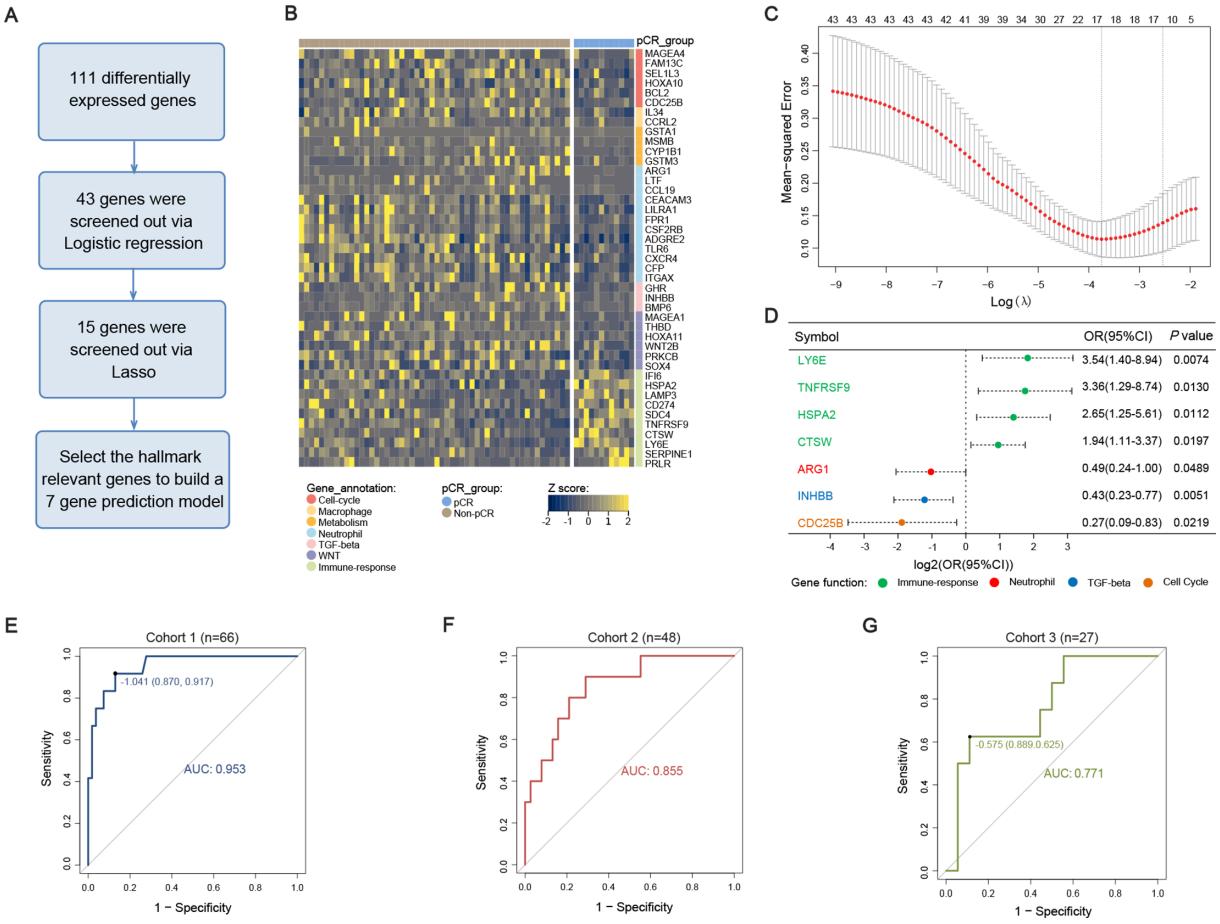


**Figure 4** Potential genes screening and prediction model construction. (A) Flowchart of model construction. (B) Heatmap depicting differential genes screened by logistic regression in cohort 1. (C) Identification of significant genes using the LASSO method. (D) Forest plot for the association between genes and pCR. (E–G) ROC curves depicting neoadjuvant chemoimmunotherapy risk prediction signature score performance in cohorts 1, 2, and 3. AUC values are shown for each cohort. Optimal cut-off values are also provided in cohorts 1 and 3. AUC, area under the ROC curve; LASSO, least absolute shrinkage and selection operator; pCR, pathological complete response; ROC, receiver operating characteristic.

in pathological response or prognosis was observed in patients receiving only nCRT (cohort 4) (online supplemental figure S7A–C) and TCGA-ESCC dataset (online supplemental figure S7D–F).

### NCIRPs outperforms PD-L1 combined positive score in predicting efficacy of neoadjuvant chemoimmunotherapy

The pCR rates in the low-risk groups were 61.1% (11/18) in cohort 1 (figure 5A,B), 50.0% (6/12) in cohort 2 (figure 5C,D), and 71.4% (5/7) in cohort 3 (figure 5E,F), respectively. While the pCR rates in the PD-L1 combined positive score (CPS) ≥1 group in cohorts 1, 2, and 3 were 28.1% (9/32) (figure 5B), 34.6% (9/26) (figure 5D), and 30.4% (7/23) (figure 5F). These results indicate that the NCIRPs is superior to PD-L1 CPS in predicting the efficacy of neoadjuvant chemoimmunotherapy.

### Synergizing NCIRPs and PD-L1 CPS increased the accuracy of predicting efficacy of neoadjuvant chemoimmunotherapy

In the combined NCIRPs and PD-L1 evaluation, the samples were classified into low-risk patients with PD-L1 CPS ≥1 (LoR&CPS ≥1) and other patients with a high risk or PD-L1 CPS <1 (other). In cohorts 1 and 2, the pCR rates in the LoR&CPS ≥1 group were further improved to 69.2% (9/13) and 60.0% (6/10), respectively (figure 5B,D). Although the number of patients was small, the pCR rate in the LoR&CPS ≥1 group in cohort 3 remained stable at 66.7% (4/6) (figure 5F). Similar results were obtained if the threshold for PD-L1 was CPS=10 (online supplemental figure S5A–C).

### NCIRPs outperforms conventional GEP biomarkers and TME subtypes in predicting efficacy of neoadjuvant chemoimmunotherapy

While comparing the NCIRPs with conventional GEP biomarkers, such as IFN-γ, chemokine, and effector T cell gene sets, AUC values for NCIRPs were considerably higher than those for other gene sets across three cohorts (online supplemental figure S5D–F). Patients with a high-risk subtype, especially in cohort 3, showed worse progression-free survival and overall survival than those in the other groups, although the p value was not significant (online supplemental figure S4B,C).

The performance of NCIRPs was compared with routinely used TME subtypes (online supplemental figure

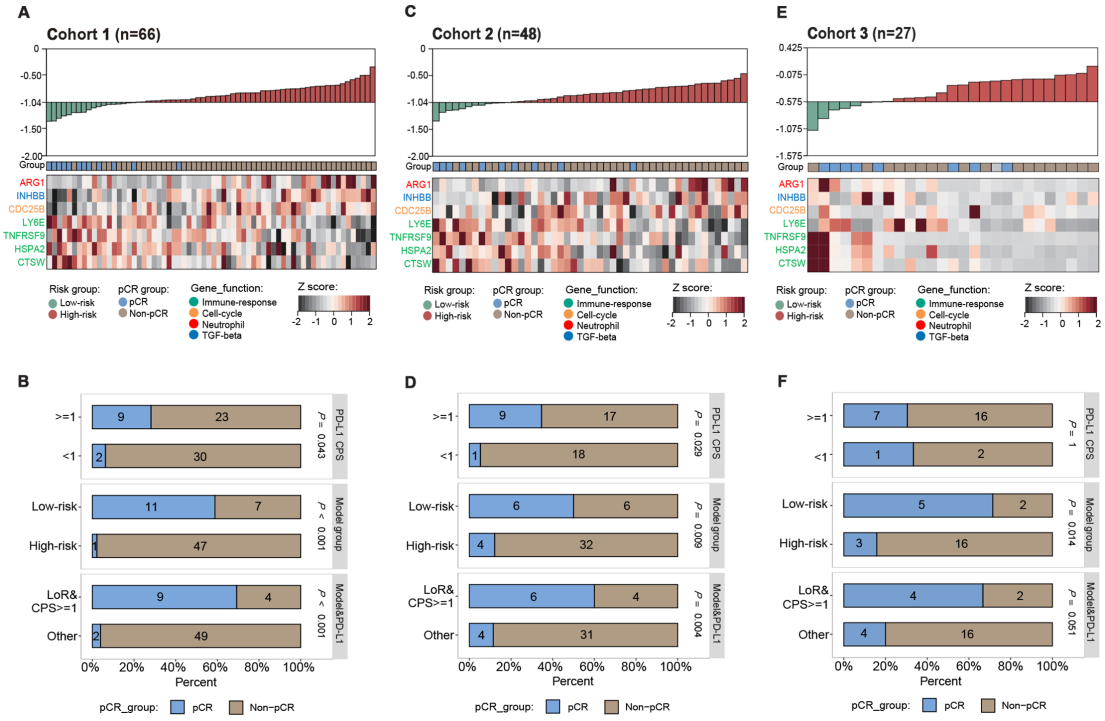


**Figure 5** NCIRPs predicts therapeutic efficacy of neoadjuvant immunotherapy in esophageal squamous cell carcinoma. (A, C, E) Risk score linkage graphs showing risk score, pCR distribution, and heatmap containing NCIRPs-related genes. (B, D, F) Stacked column graphs illustrating the distribution of non-pCR and pCR patients across risk prediction, PD-L1 CPS, and combination groups. CPS, combined positive score; NCIRPs, neoadjuvant chemoimmunotherapy risk prediction signature; pCR, pathological complete response; PL-D1, programmed death ligand 1.

S6A–E). The pCR rates in the ImmHot group were 26.7% (8/30), 33.3% (7/21), and 36.4% (4/11) in cohorts 1, 2, and 3, respectively, which were all lower than those in the low-risk group of the corresponding cohort (online supplemental figure S5G–I).

### Model defined high-risk ESCC associated with immune-suppressive context of TME

According to the evaluation of tumor immune infiltration in different risk groups, immune infiltration in the low-risk group was higher than that in cohorts 1 and 2 (figure 6A,D). The correlation analysis results showed a negative correlation between the NCIRPs score and immune activation features, such as T cells, NK cells, and checkpoint molecules in cohorts 1 and 2 (figure 6C,F), as well as B and T cells in cohort 3 (online supplemental figure S4D,E).

The state of immune infiltrate differed significantly between low- and high-risk patients, with over-representation of IE and IE/F subtypes in low-risk patients and over-representation of D and F subtypes in high-risk patients (figure 6B,E). Thus, low-risk patients predicted by the NCIRPs exhibited immune activation, while high-risk patients showed signs of immune suppression.

## DISCUSSION

Like previous studies, the present research demonstrated that neoadjuvant chemoimmunotherapy has favorable safety and efficacy in the treatment of ESCC. The pCR rates varied from 20% to 39.2% in different studies.[11 12 14] The present study represents the largest sample size reported to date for neoadjuvant chemoimmunotherapy for ESCC. The pCR rate was ~20%. Predicting pCR in ESCC is crucial as it relates to the strategy of operation or organ preservation treatment. Currently, there are no reliable biomarkers to predict pCR or treatment efficacy.

Previous studies have not reached a consensus on the relevance of tumor immune microenvironment for efficacy.[11 15] However, the present study clarified that the immune microenvironment is a clear contributor to efficacy and response. It also revealed that immune-enriched TME characterized by NK infiltration and activated $CD4^+$ cells was associated with a positive response to neoadjuvant chemoimmunotherapy, particularly in achieving a pCR. Neutrophils, which have recently received increased attention in cancer research, play a critical role in cancer development and progression. Cytokine and epigenetic regulation in the microenvironment induce neutrophils to polarize into either TAN1 or TAN2. The present study indicated that patients in the non-pCR group had a higher expression of TAN2. The study also revealed that neutrophil infiltration, especially that of TAN2, was associated with therapeutic resistance in ESCC. Promoting the polarization of neutrophils from tumor-promoting phenotype (TAN2) to antitumor phenotype (TAN1) may be a potential therapeutic strategy to enhance the efficacy of neoadjuvant chemoimmunotherapy.

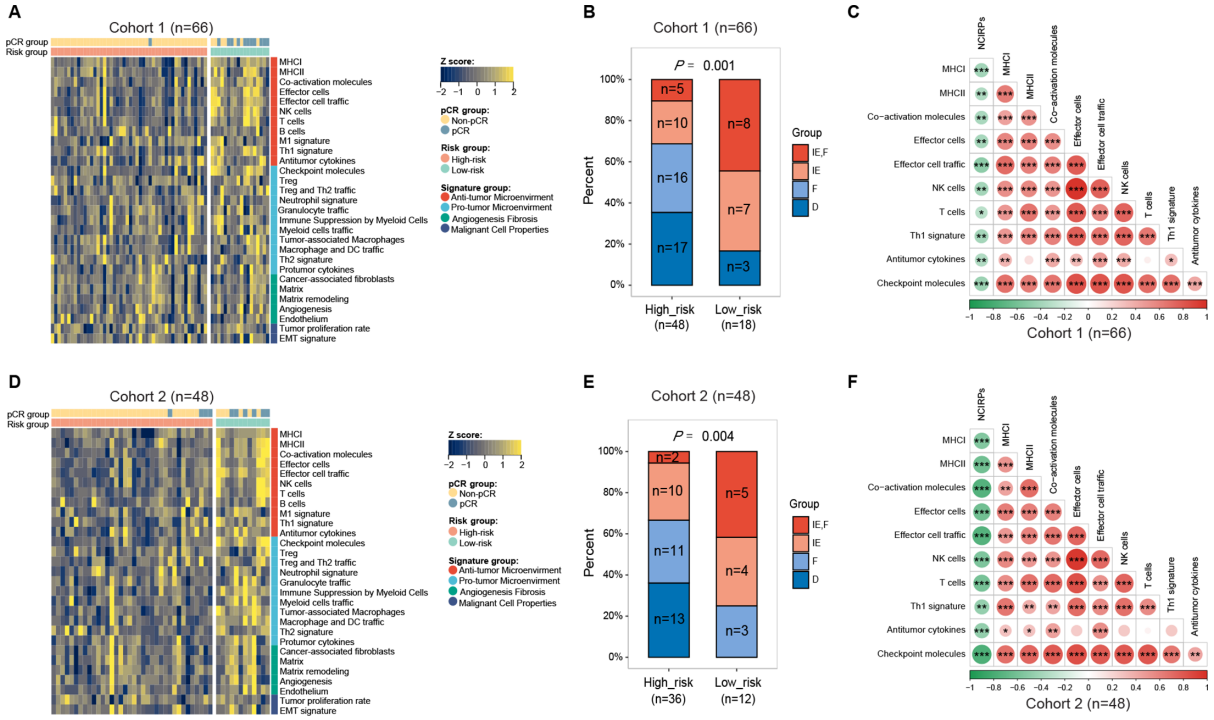


**Figure 6** Characterization of tumor microenvironment (TME) status of different risk groups. (A, D) Heatmaps illustrating 29-gene expression signatures related to TME. (B, E) Stacked column graphs illustrating the distribution of different TME subtypes in groups with different risk prediction scores across cohorts 1 and 2. IE,F, immune-enriched, fibrotic; IE, immune-enriched; F, fibrotic; D, depleted. (C, F) Correlation maps and heatmaps analyzing the association between NCIRPs and gene expression signatures. Dot color represents the Pearson correlation coefficient, and dot size represents the absolute value of the correlation coefficient. *, **, and *** represent statistical significance levels of p<0.05, p<0.01, and p<0.001, respectively.

A previous study has reported that combined $CD4^+$ T cells and the expression levels of IFN-γ, LAMP3, or Gal.1 in serum can distinguish responders from non-responders among patients with locally advanced ESCC who received neoadjuvant chemoimmunotherapy. However, this study did not demonstrate the predictive efficacy of these biomarkers for pCR, and there was no further validation from an external validation set.[15] Another study has reported on a potential response biomarker "IFN/EMT score" for ESCC patients who received neoadjuvant anti-PD-L1 antibody monotherapy based on frozen samples. However, its application in routine practice requires further evaluation, and the pCR rate in the study was only 8%, indicating that neoadjuvant anti-PD-L1 antibody monotherapy had a limited therapeutic value.[32]

In the present study, the NCIRPs model was discovered, trained, and validated in a large sample population. Its specificity for immunotherapy efficacy was reverse-validated using TCGA and neoadjuvant radiotherapy cohorts. This is the first model of its kind that is stable and clinically valuable. Compared with predefined immune signatures, such as those of T effector cells, chemokines, and IFN-γ genes, the present model uses fewer genes to accurately predict pCR in ESCC patients receiving neoadjuvant chemoimmunotherapy. Additionally, this model has an advantage over the PD-L1 CPS score. Encouragingly, the combination of PD-L1 CPS score and NCIRPs significantly enhances the predictive accuracy for pCR, providing a favorable prediction tool for selecting the right patients for neoadjuvant chemoimmunotherapy.

Moreover, genes in the prognostic algorithm have interpretable functions. CTSW exhibits a remarkably restricted cellular pattern of expression, being predominantly expressed in cytotoxic T and NK cells.[33–35] TNFRSF9, also known as CD137, is a novel potential target for enhancing antitumor immune responses that is widely expressed in a variety of immune cells, including activated $CD4^+$ and $CD8^+$ T cells, regulatory T cells, NK cells, NKT cells, and dendritic cells. TNFRSF9 agonists in combination with anti-PD-1 antibody can effectively activate and amplify tumor-specific cytotoxic T cells to enhance tumor killing.[36 37] LY6E, which was initially identified in a mouse thymus, has been reported to be related to immune regulation, especially in promoting T cell proliferation, development, and activation.[38] HSPA2 is a member of the HSPA (HSP70) chaperone family that can enhance the immunogenicity of apoptotic tumor cells and stimulate anti-tumor immunity mediated by T cells.[39] On the other hand, ARG1, which is known as a metabolic enzyme degrading arginine expressed by immunomodulatory cells including M2-like tumor-associated macrophages and regulatory T cells, can suppress antitumor immunity by limiting the availability of arginine to T cells.[40 41] ARG1-expressing TANs are immunosuppressive and, as a result, tumor-promoting for multiple cancer types.[23] Although limited studies have shown that

CDC25B is associated with immune regulation, cell-cycle regulator CDC25B has been found to be an oncogene that promotes ESCC cell proliferation and invasion[42] and predicts poor prognosis for ESCC patients.[43] INHBB is a glycoprotein that belongs to the TGF-β family. It has been reported that it affects the development and prognosis of different tumors and contributes to immune infiltration to promote gastric cancer development.[44] The present study found that INHBB was relatively more expressed in immune-unfavorable TME subtypes compared with immune-favorable TME subtypes and was associated with immune suppression in ESCC. Although higher INHBB expression has been reported in esophageal squamous dysplasia than in normal mucosa,[45] the role of INHBB in ESCC needs a further exploration. The present study also validated the biological significance of NCIRPs using mIF and TME subtype evaluation. The consistency and reproducibility of the present study findings reinforce the NCIRPs as a promising model to predict the effectiveness of neoadjuvant chemoimmunotherapy.

There are also some limitations in this study. First, the study follow-up period was limited, and a longer follow-up is needed to confirm the predictive value of NCIRPs for the survival outcome of ESCC patients receiving neoadjuvant chemoimmunotherapy. Second, prospective trials are necessary to validate the predictive power of the model. Third, the role of model genes in immunotherapy and their indications of novel therapeutic regimens will require further validations using ex vivo and in vitro models. Furthermore, we conducted an initial analysis of drug sensitivity data to pinpoint compounds capable of reclassifying patients from high-risk to low-risk categories. This included a focus on agents such as protein kinase C inhibitors and histone deacetylase inhibitors. However, given that these findings are preliminary and derived solely from database analysis, they lack the depth required for inclusion in this paper, which can be based on the further validated data to be shown in the subsequent study.

In conclusion, the present study disclosed the hallmarks of therapeutic efficacy regarding neoadjuvant chemoimmunotherapy in ESCC. Based on the discovered hallmarks, NCIRP was constructed displaying more efficient in distinguishing patients of pCR and non-pCR compared with PD-L1, TME phenotypes, and other conventional immune signatures. The combination of the NCIRPs and PD-L1 was more effective in identifying patients who could benefit from the neoadjuvant chemoimmunotherapy treatment.

**Author affiliations**
[1]Department of Pathology, Zhejiang Cancer Hospital, Hangzhou, Zhejiang, China
[2]Medical Department, Amoy Diagnostics Co Ltd, Xiamen, Fujian, China
[3]Department of Pulmonary Surgery, Zhejiang Cancer Hospital, Hangzhou, Zhejiang, China
[4]Cancer Research Institute, Zhejiang Cancer Hospital, Hangzhou, Zhejiang, China
[5]Department of Pathology, Taizhou Hospital of Zhejiang Province affiliated with Wenzhou Medical University, Taizhou, Zhejiang, China
[6]Department of Clinical Laboratory, Zhejiang Cancer Hospital, Hangzhou, Zhejiang, China

**Correction notice** This article has been corrected since it was first published. The last author's correspondence email address has been updated.

**Acknowledgements** We also thank TissueGnostics Asia Pacific limited (Beijing, China) for their technical support in multiplexed immunofluorescence staining, image scanning and analysis, and the help of technical engineer Xiaojing Liu.

**Contributors** TF and QL were involved in data curation, analysis, visualization, writing, review, and editing. RZ contributed to data curation, analysis, and interpretation. CZ contributed to conceptualization, data analysis, manuscript writing, and editing. DS and QC conceived the study. CY, LX, LY, CW, WX, JW, JZ, MH, CX, JJ, XZ, TL, and YY were involved in clinical data generation and curation and discussion. All authors approved the article for submission and publication. Responsible for the overall content as guarantors: DS and QC.

**Funding** This work was supported by National Key Research and Development Program of China (2021YFA0910100 and 2021YFA0910101), the Major Science and Technology Project of Medical and Health of Zhejiang Province of China (WKJ-ZJ-2402), National Natural Science Foundation of China (No. 81972917).

**Competing interests** CZ, QL, and XZ were employed by Amoy Diagnostics Co., Ltd. All other authors declare no competing interests.

**Patient consent for publication** Not applicable.

**Ethics approval** This study involves human participants and the study was approved by the Medical Ethics Committee of Zhejiang Cancer Hospital (IRB-2021-348). Informed consent of the patients was exempted due to the retrospective nature of the study.

**Provenance and peer review** Not commissioned; externally peer reviewed.

**Data availability statement** Data are available upon reasonable request.



**ORCID iD**
Dan Su http://orcid.org/0000-0002-8423-1994

## REFERENCES

1 Yang H, Liu H, Chen Y, *et al*. Neoadjuvant Chemoradiotherapy Followed by Surgery Versus Surgery Alone for Locally Advanced Squamous Cell Carcinoma of the Esophagus (NEOCRTEC5010): A Phase III Multicenter, Randomized, Open-Label Clinical Trial. *J Clin Oncol* 2018;36:2796–803.
2 van Hagen P, Hulshof MCCM, van Lanschot JJB, *et al*. Preoperative chemoradiotherapy for esophageal or junctional cancer. *N Engl J Med* 2012;366:2074–84.
3 Sun J-M, Shen L, Shah MA, *et al*. Pembrolizumab plus chemotherapy versus chemotherapy alone for first-line treatment of advanced oesophageal cancer (KEYNOTE-590): a randomised, placebo-controlled, phase 3 study. *Lancet* 2021;398:759–71.
4 Doki Y, Ajani JA, Kato K, *et al*. Nivolumab Combination Therapy in Advanced Esophageal Squamous-Cell Carcinoma. *N Engl J Med* 2022;386:449–62.
5 Luo H, Lu J, Bai Y, *et al*. Effect of Camrelizumab vs Placebo Added to Chemotherapy on Survival and Progression-Free Survival in Patients With Advanced or Metastatic Esophageal Squamous Cell Carcinoma: The ESCORT-1st Randomized Clinical Trial. *JAMA* 2021;326:916–25.

6 Wang Z-X, Cui C, Yao J, *et al*. Toripalimab plus chemotherapy in treatment-naïve, advanced esophageal squamous cell carcinoma (JUPITER-06): A multi-center phase 3 trial. *Cancer Cell* 2022;40:277–88.
7 Lu Z, Wang J, Shu Y, *et al*. Sintilimab versus placebo in combination with chemotherapy as first line treatment for locally advanced or metastatic oesophageal squamous cell carcinoma (ORIENT-15): multicentre, randomised, double blind, phase 3 trial. *BMJ* 2022;377:e068714.
8 Xu J, Kato K, Raymond E, *et al*. Tislelizumab plus chemotherapy versus placebo plus chemotherapy as first-line treatment for advanced or metastatic oesophageal squamous cell carcinoma (RATIONALE-306): a global, randomised, placebo-controlled, phase 3 study. *Lancet Oncol* 2023;24:483–95.
9 Kelly RJ, Ajani JA, Kuzdzal J, *et al*. Adjuvant Nivolumab in Resected Esophageal or Gastroesophageal Junction Cancer. *N Engl J Med* 2021;384:1191–203.
10 Duan H, Shao C, Pan M, *et al*. Neoadjuvant Pembrolizumab and Chemotherapy in Resectable Esophageal Cancer: An Open-Label, Single-Arm Study (PEN-ICE). *Front Immunol* 2022;13:849984.
11 Yang W, Xing X, Yeung S-CJ, *et al*. Neoadjuvant programmed cell death 1 blockade combined with chemotherapy for resectable esophageal squamous cell carcinoma. *J Immunother Cancer* 2022;10:e003497.
12 Liu J, Yang Y, Liu Z, *et al*. Multicenter, single-arm, phase II trial of camrelizumab and chemotherapy as neoadjuvant treatment for locally advanced esophageal squamous cell carcinoma. *J Immunother Cancer* 2022;10:e004291.
13 Yan X, Duan H, Ni Y, *et al*. Tislelizumab combined with chemotherapy as neoadjuvant therapy for surgically resectable esophageal cancer: A prospective, single-arm, phase II study (TD-NICE). *Int J Surg* 2022;103:106680.
14 Chen X, Xu X, Wang D, *et al*. Neoadjuvant sintilimab and chemotherapy in patients with potentially resectable esophageal squamous cell carcinoma (KEEP-G 03): an open-label, single-arm, phase 2 trial. *J Immunother Cancer* 2023;11:e005830.
15 Zhang G, Yuan J, Pan C, *et al*. Multi-omics analysis uncovers tumor ecosystem dynamics during neoadjuvant toripalimab plus nab-paclitaxel and S-1 for esophageal squamous cell carcinoma: a single-center, open-label, single-arm phase 2 trial. *EBioMedicine* 2023;90:104515.
16 Bagaev A, Kotlov N, Nomie K, *et al*. Conserved pan-cancer microenvironment subtypes predict response to immunotherapy. *Cancer Cell* 2021;39:845–65.
17 Liu Z, Zhao Y, Kong P, *et al*. Integrated multi-omics profiling yields a clinically relevant molecular classification for esophageal squamous cell carcinoma. *Cancer Cell* 2023;41:181–95.
18 Dobin A, Davis CA, Schlesinger F, *et al*. STAR: ultrafast universal RNA-seq aligner. *Bioinformatics* 2013;29:15–21.
19 Li B, Dewey CN. RSEM: accurate transcript quantification from RNA-Seq data with or without a reference genome. *BMC Bioinformatics* 2011;12:323.
20 Li Y, Ge X, Peng F, *et al*. Exaggerated false positives by popular differential expression methods when analyzing human population samples. *Genome Biol* 2022;23:79.
21 Wu T, Hu E, Xu S, *et al*. clusterProfiler 4.0: A universal enrichment tool for interpreting omics data. *Innov Camb* 2021;2:100141.
22 Subramanian A, Tamayo P, Mootha VK, *et al*. Gene set enrichment analysis: a knowledge-based approach for interpreting genome-wide expression profiles. *Proc Natl Acad Sci U S A* 2005;102:15545–50.
23 Jaillon S, Ponzetta A, Di Mitri D, *et al*. Neutrophil diversity and plasticity in tumour progression and therapy. *Nat Rev Cancer* 2020;20:485–503.
24 Keeley T, Costanzo-Garvey DL, Cook LM. Unmasking the Many Faces of Tumor-Associated Neutrophils and Macrophages: Considerations for Targeting Innate Immune Cells in Cancer. *Trends Cancer* 2019;5:789–98.
25 Barbie DA, Tamayo P, Boehm JS, *et al*. Systematic RNA interference reveals that oncogenic KRAS-driven cancers require TBK1. *Nature New Biol* 2009;462:108–12.
26 Bindea G, Mlecnik B, Tosolini M, *et al*. Spatiotemporal dynamics of intratumoral immune cells reveal the immune landscape in human cancer. *Immunity* 2013;39:782–95.
27 Hänzelmann S, Castelo R, Guinney J. GSVA: gene set variation analysis for microarray and RNA-seq data. *BMC Bioinformatics* 2013;14:7.
28 Cristescu R, Mogg R, Ayers M, *et al*. Pan-tumor genomic biomarkers for PD-1 checkpoint blockade-based immunotherapy. *Science* 2018;362:eaar3593.
29 Jiang P, Gu S, Pan D, *et al*. Signatures of T cell dysfunction and exclusion predict cancer immunotherapy response. *Nat Med* 2018;24:1550–8.
30 Ayers M, Lunceford J, Nebozhyn M, *et al*. IFN-γ-related mRNA profile predicts clinical response to PD-1 blockade. *J Clin Invest* 2017;127:91190:2930–40:.
31 Zhang Z, Li Q, Sun S, *et al*. Prognostic and immune infiltration significance of ARID1A in TCGA molecular subtypes of gastric adenocarcinoma. *Cancer Med* 2023;12:16716–33.
32 Yin J, Yuan J, Li Y, *et al*. Neoadjuvant adebrelimab in locally advanced resectable esophageal squamous cell carcinoma: a phase 1b trial. *Nat Med* 2023;29:2068–78.
33 Stoeckle C, Gouttefangeas C, Hammer M, *et al*. Cathepsin W expressed exclusively in CD8+ T cells and NK cells, is secreted during target cell killing but is not essential for cytotoxicity in human CTLs. *Exp Hematol* 2009;37:266–75.
34 Brinkworth RI, Tort JF, Brindley PJ, *et al*. Phylogenetic relationships and theoretical model of human cathepsin W (lymphopain), a cysteine proteinase from cytotoxic T lymphocytes. *Int J Biochem Cell Biol* 2000;32:373–84.
35 Wex T, Bühling F, Wex H, *et al*. Human cathepsin W, a cysteine protease predominantly expressed in NK cells, is mainly localized in the endoplasmic reticulum. *J Immunol* 2001;167:2172–8.
36 Cappell KM, Kochenderfer JN. A comparison of chimeric antigen receptors containing CD28 versus 4-1BB costimulatory domains. *Nat Rev Clin Oncol* 2021;18:715–27.
37 Kraehenbuehl L, Weng C-H, Eghbali S, *et al*. Enhancing immunotherapy in cancer by targeting emerging immunomodulatory pathways. *Nat Rev Clin Oncol* 2022;19:37–50.
38 Yu J, Liu SL. Emerging Role of LY6E in Virus-Host Interactions. *Viruses* 2019;11:1020.
39 Feng H, Zeng Y, Graner MW, *et al*. Exogenous stress proteins enhance the immunogenicity of apoptotic tumor cells and stimulate antitumor immunity. *Blood* 2003;101:245–52.
40 Arlauckas SP, Garren SB, Garris CS, *et al*. Arg1 expression defines immunosuppressive subsets of tumor-associated macrophages. *Theranostics* 2018;8:5842–54.
41 Zhang X, Ji L, Li MO. Control of tumor-associated macrophage responses by nutrient acquisition and metabolism. *Immunity* 2023;56:14–31.
42 Wang M, Wang L, Zhang M, *et al*. MiR-214 inhibits the proliferation and invasion of esophageal squamous cell carcinoma cells by targeting CDC25B. *Biomed Pharmacother* 2017;95:1678–83.
43 Dong J, Zeng B, Xu L, *et al*. Anti-CDC25B autoantibody predicts poor prognosis in patients with advanced esophageal squamous cell carcinoma. *J Transl Med* 2010;8:81.
44 Yu W, He G, Zhang W, *et al*. INHBB is a novel prognostic biomarker and correlated with immune infiltrates in gastric cancer. *Front Genet* 2022;13:933862.
45 Joshi N, Johnson LL, Wei W-Q, *et al*. Gene expression differences in normal esophageal mucosa associated with regression and progression of mild and moderate squamous dysplasia in a high-risk Chinese population. *Cancer Res* 2006;66:6851–60.